Journal of Applied Polymer Science

Effect of Clay Type and Polymer Matrix on Microstructure and Tensile Properties of PLA/LLDPE/Clay Nanocomposites

Ladan As'habi,[1] Seyed Hassan Jafari,[1] Hossein Ali Khonakdar,[2] Bernd Kretzschmar,[3] Udo Wagenknecht,[3] Gert Heinrich[3]

[1]School of Chemical Engineering, College of Engineering, University of Tehran, 11155-4563, Tehran, Iran
[2]Department of Plastic Processing, Iran Polymer and Petrochemical Institute, 14965-115, Tehran, Iran
[3]Department of Processing, Leibniz Institute of Polymer Research Dresden, Hohe Str. 6, D-01069, Dresden, Germany
Correspondence to: S. H. Jafari (E-mail: shjafari@ut.ac.ir)

ABSTRACT: Polylactide (PLA)/linear low-density polyethylene (LLDPE), (PLA/LLDPE), blends and nanocomposites were prepared by melt mixing process with a view to fine tune the properties. Two different commercial-grade nanoclays, Cloisite® 30B (30B) and Cloisite® 15A (15A) were used. A terpolymer of ethylene, butylacrylate (BA) and glycidylmethacrylate (GMA) was used as a reactive compatibilizer. The influence of type of clay on the morphology and mechanical properties of two PLA-rich and LLDPE-rich blend systems was studied. Morphological analysis using X-ray diffraction, transmission electron microscopy, and scanning electron microscopy revealed that the organoclay layers were dispersed largely at the interface of PLA/LLDPE. Decreasing the PLA content changed the morphology from droplet-in matrix to coarse co-continuous. In comparison with 30B, due to less affinity of 15A towards compatibilizer and PLA phase, the reduction of the size of dispersed phase was less than that of the equivalent 30B composites. The mechanical results demonstrated that the composites containing both types of organoclay exhibited higher modulus but lower elongation and tensile strength as compared to the neat blends. The injection molded nanocomposites were shown to have the sequential fracture behavior during tensile test. The tensile testing results on the neat blends and nanocomposites showed significant increase in elongation at break and decrease in the modulus as compared with the neat PLA. © 2013 Wiley Periodicals, Inc. J. Appl. Polym. Sci. 130: 749–758, 2013

KEYWORDS: morphology; mechanical properties; polyolefins; blends

Received 27 April 2012; accepted 24 February 2013; published online 2 April 2013
DOI: 10.1002/app.39209

INTRODUCTION

Polymers from renewable resources have gained much attention over the last two decades, mainly due to two major reasons: first, limitation of fossil fuel resources, and second, environmental concerns. As one of the biodegradable polymers, poly (lactic acid) or polylactide (PLA) has attracted an increasing attention due to its comprehensive mechanical properties and its potential to replace conventional petrochemical-based polymers. PLA is a linear aliphatic polyester that can be semicrystalline or totally amorphous, depending on the stereopurity of the polymer backbone. In general most of the commercial PLA grades are semicystalline and contain less than 6% D-lactide. The properties of PLA such as degradability, mechanical and thermal properties, are strongly dependent on the degree of crystallinity.[1] Because of high stiffness, modulus and strength of PLA, it has been used in many applications such as food packagings, films, and textiles. However, some of the other properties such as heat distortion temperature (HDT), melt strength, impact resistance, gas barrier properties, etc. are not good enough for various end-use applications such as packaging.[2]

In recent years, considerable efforts have been made to improve the brittleness, thermal properties and gas barrier properties by blending PLA with other polymers, low molecular weight plasticizers or with the intercalation of PLA in the silicate galleries of nanoclay to prepare nanocomposite systems with superior properties.[3]

Among the petrochemical-based polymer, polyethylene (PE) is one of the most consumed polymers in the packaging industry. Considering the low price and good mechanical properties of PE, it can be a good candidate for improving the toughness of PLA. Only limited researches on PLA/PE exists in the literature. In addition, this blend system has attracted many interests because it complements brittleness of the PLA. Studies have shown that blending of PLA with linear low-density

polyethylene (LLDPE) resulted in significant increase in PLA ductility and toughness but the PLA strength and modulus were also substantially reduced.[4–10] Because of the immiscibility of this polymer pair, several researchers employed different compatibilizer to further tailoring their properties.

Anderson et al. showed that for the amorphous PLA the toughening was achieved only when a poly (L-lactide) (PLLA)-PE block copolymer was used as compatibilizer.[4] On the other hand Kim et al. investigated blends of PLLA and low-density polyethylene (LDPE) and found that the domain size of dispersed phase decreased and the tensile properties enhanced significantly by using a reactive compatibilizer having glycidyl methacrylate (GMA) functional group.[5] Rezgui et al. studied the plastic deformation and modeled the creep behavior of LDPE reinforced with PLA.[7,8] They pointed out that the deformation damage of LDPE/PLA blends increased with increasing the PLA content.[7] They also found that with increasing concentrations of PLA, the blend showed higher Young's modulus, stiffer viscoelastic response, and earlier fracture.[8] Recently Nuñez et al. studied the PLA/LLDPE nanocomposites based on sepiolite.[9] They showed that the compatibilized blends prepared without clay have higher thermal degradation susceptibility and tensile toughness than those prepared with sepiolite. Moreover significant changes in complex viscosity and melt elasticity values were observed on sepiolite incorporation. This blend nanocomposites exhibited similar thermal degradation, lower tensile strength, and Young's modulus values and increased elongation at break and tensile toughness, complex viscosity, and storage modulus compared with the nanocomposite of PLA.

Thermal properties and degradation characteristic of PLA/LLDPE was also studied by Singh et al.[10,11] They found that the degradation in alkaline medium and the presence of compatibilizer was favorable. In addition among the investigated samples the compatibilized blends with higher content of LLDPE (80 wt %) showed better mechanical and thermal properties.

Hydrolysis degradation behavior of starch/LDPE and starch/LDPE/PLLA blend systems was also studied in acidic solution.[12] Raghavan et al. studied the micro-structure of starch/LDPE/PLLA/vernonia oil. According to the results the vernonia oil was present at the interface of the starch/polyethylene. They also showed that the quantity of water passing through the porous acid hydrolyzed composite depended on the thickness of the film.

Besides these studies on PLA/PE blends, there are several reports on PLA blend nanocomposites.[13–22] These studies mainly focused on the study of thermal, mechanical, and permeability properties of PLA/poly caprolactone (PCL) nanocomposites,[13–16] the rheological behavior of PLA/poly(butylene succinate) (PBS) nanocomposites[17–19] and the mechanical and rheological behavior of PLA/poly(butylene adipate-*co*-terephthalate) (PBAT) nanocomposites.[20–22] In our previous work we reported on the effect of mixing sequence on rheological behavior as well as biodegradation properties of the PLA/LLDPE/clay system.[23] This work is focused mainly on the influence of clay type and clay content on the state of clay dispersion as well as their consequent effects on morphology and mechanical properties of the compatibilized PLA/LLDPE system. The addition of compatibilizer to a clay-containing multiphase system can have its own contribution towards clay positioning and dispersion due to imposed changes on the system thermodynamics. This issue has been discussed intensively in the literature,[24–26] and therefore, it will not be addressed again in this work. No comparison was made between compatibilized and noncompatibilized systems. In this study the microstructure and tensile properties of different nanocomposite systems based on PLA/LLDPE blends by two approaches were investigated to achieve PLA composites with better-balanced properties. In PLA-rich system the brittleness of PLA was improved with LLDPE, as one of the most widely used commodity plastics. In LLDPE-rich system, PLA has chosen as a counterpart of LLDPE due to its biodegradable properties. Blends and nanocomposites of LLDPE and PLA may be a candidate for excellent biodegradable and inexpensive packaging materials. The Cloisite 30B was chosen due to the polar nature of PLA and better affinity between this nanoclay and PLA. A nonpolar organoclay-like Cloisite 15A with long alkyl tail surfactant was used for LLDPE matrices. This study illustrates a new approach to achieve PLA composites with better-balanced properties.

EXPERIMENTAL

Materials and Sample Preparation

The PLA used in this study was a commercial grade NatureWorks® PLA 4042D, containing 4.5% of D-Lactide, supplied by NatureWorks (USA). The linear low density polyethylene (LLDPE) used was also a commercial grade (LL 4004EL) supplied by ExxonMobile Chemicals (USA), having a melt flow index of 3.6 g/10 min (190°C, 2.16 kg). The Elvaloy® PTW which is a terpolymer of ethylene, n-butylacrylate (BA) and glycidylmethacrylate (GMA) with MFI of 12 g/10 min (190°C, 2.16 kg) supplied by DuPont (USA) used as a reactive compatibilizer. Two different organo-modified clays (Southern Clay Products) Cloisite®30B, (30B), MMT-Na+ modified with bis-(2-hydroxyethyl) methyl tallowalkyl ammonium cations and Cloisite® 15A, (15A), MMT-Na+ modified with dimethyl, dehydrogenated tallow, quaternary ammonium cations were used in this study. Before mixing, all the polymers and the organo-modified clays (OMMT) were dried in a vacuum oven at 80°C for 24 h.

A corotating twin-extruder (ZSK 30) equipped with gravimetric feeders and a strand pelletizer was employed to compound the blends as well as nanocomposites. The screw speed of 150 rpm and the feed rate of 10 kg/h were used for all runs. The extrusion temperature profile was set from 160 to 190°C from hopper to die. The blend and nanocomposite pellets were then dried in a vacuum oven at 80°C for 24 h prior to characterization and testing. The compatibilized blend and nanocomposites had about 5 wt % compatibilizer. The OMMT loading in each nanocomposite samples was about 3 wt % of the total mixture (Table I).

Characterization

Wide-angle X-ray scattering (WAXS) patterns were recorded using Co K_α radiation (40 kV, 40 mA) generated by an X-ray diffractometer (Xpert, Philips); corresponding data were

Table I. Sample Composition

Sample	Composition (wt %)				
	PLA	LLDPE	Cloisite 30B	Cloisite 15A	Elvaloy
PLA71/LLDPE24	71	24	-	-	5
PLA24/LLDPE71	24	71	-	-	5
PLA69/LLDPE23/30B	69	23	3	-	5
PLA69/LLDPE23/15A	69	23	-	3	5
PLA23/LLDPE69/30B	23	69	3	-	5
PLA/LLDPE/15A	23	69	-	3	5

collected from 2θ angle of 1.5° to 10° to characterize the spacing of the layer structure of the neat OMMT as well as that of the nanocomposite samples in the form of sheets. The scanning rate was 1°/min with a step size of 0.02°.

The dispersion of the OMMT platelets in the blend was studied by means of transmission electron microscopy (TEM). The samples were cut by cryo-ultramicrotom from extruded bars in thin section (~ 60 nm thick) at −120°C using a diamond knife. The sections were observed by means of a Carl Zeiss LIBRA® 200 CS-STEM, using an accelerated voltage of 200 kV. The clear contrast between PLA and LLDPE are observable, due to high electron density difference between the phases.

Scanning electron microscopy (SEM) was used to characterize the morphology of the blends and nanocomposites. The surfaces were prepared by cryo-fracturing at the tensile direction (i.e., melt flow direction in injection molding) for analyzing any occurrence of microstructure anisotropy. The ultra-thin sections which were prepared from the cross section of all samples compared with each other.

All specimens after proper drying were sputter coated with gold prior to examination and observed under a VEGA TESCAN.

Standard tensile test samples (ISO 527-1) were prepared by injection molding operated at 190 °C with the mold temperature of 30°C. After molding, the molded specimens were conditioned at room temperature for at least 24 h to allow for any relaxation of elasticity within the specimens.

The tensile testing was performed on a tensile tester (Zwick/Roell, Germany) according to the standard method for testing the tensile properties of rigid plastics (ISO 527-1:1993) at room temperature. For all samples the crosshead speed was 50 mm/min and the average values of at least seven measurements were reported.

RESULTS AND DISCUSSION

X-ray Diffraction

The level of intercalation and exfoliation of the organoclay was investigated using X-ray diffraction (XRD) technique. The XRD patterns for PLA/LLDPE nanocomposites are shown in Figure 1. The XRD patterns of the neat organoclays were also recorded as reference. The mean interlayer spacing for the 30B organoclay is 18.45 A° corresponding to 2θ =4.85°. In the case of PLA69/LLDPE23/30B (PLA-rich system) a small shifted peak is observed at 2θ =3° (corresponding to a basal spacing of 34 A°) [Figure 1(a)], representing intercalated structure. The LLDPE-rich system (PLA23/LLDPE69/30B) in Figure 1(a) has also an intercalated morphology. This sample shows a similar peak at 3° with basal spacing of 34A°. Similar diffraction peaks are observed for both PLA-rich and LLDPE-rich systems having different PLA contents. In other words the ability of these two matrixes to swell the organoclay crystallites is similar.

Figure 1(b) shows the mean interlayer spacing of 15A and the related nanocomposite systems based on this type of clay. The mean interlayer spacing of 15A is 30.9 A° at 2θ = 2.77°. In the case of blends with 3 wt % 15A, no significant peak shift was observed. In the 15A based blend nanocomposites unlike the 30B-based nanocomposites, the *d*-spacing of silicate layers differs only slightly from that of neat 15A. Similar results have been reported by other researchers.[27] The small peaks which are observed at 2θ =5.6° in the 15A-based nanocomposites are related to the (002) plane of the silicate layers dispersed in the matrix.[28] The difference in the phase morphology of two kinds of clay nanocomposites can be explained from the chemical component and structure of organic surfactants used in 30B and 15A. Different cationic modifiers present on the clay surfaces result in different polarity and interlayer gallery of organoclay. This leads to a different level of intercalation or exfoliation in polymer matrix. Generally, polar organoclay from a surfactant with only one long alkyl (i.e., 30B) can be used to modify polar polymer, like PLA; on the other hand, nonpolar organoclay from two or more long alkyl tail surfactant (i.e., 15A) may be used to modify the polymer like polyolefin matrices. Therefore, the results confirm that the structure of clay modifier is one of the most important factors that can influence the level of dispersion of nanoclays. Similar to [Figure 1(a)], the basal spacing of the organoclay is unaffected by the PLA content, and it is 35.6 A° for PLA contents of 23 and 69 wt %.

Microscopic Analyses Using TEM and SEM

For a qualitative understanding of the internal structure of the nanocomposite systems TEM was used. Combination of XRD and TEM is useful for a precise result. TEM micrographs of PLA/LLDPE nanocomposites with different magnifications are illustrated in Figures 2 and 3. The typical two-phase structure can be seen in these TEM micrographs, in which the dark grey parts are PLA phase and the white parts correspond to LLDPE phase. The dark lines are the cross section of the clay layers that have been delaminated and dispersed in the polymer matrix.

The TEM images for PLA69/LLDPE23/30B-based nanocomposites presented in Figure 2(a–c) are indicative of an intercalated/exfoliated structure. Some partly exfoliated clay platelets are located at the interface between PLA and LLDPE. But, besides the exfoliated organoclay layers, some organoclay stack are also visible mostly in the PLA phase [Figure 2(a,c)]. Presence of these stacks was earlier confirmed by the XRD results. It can be seen from Figure 2(a–c) that the main part of nanoclay is localized at the interface between PLA and LLDPE. This implies that the adsorbed compatibilizer macromolecules on clay surface are desorbed by PLA macromolecules. Since the compatibilizer

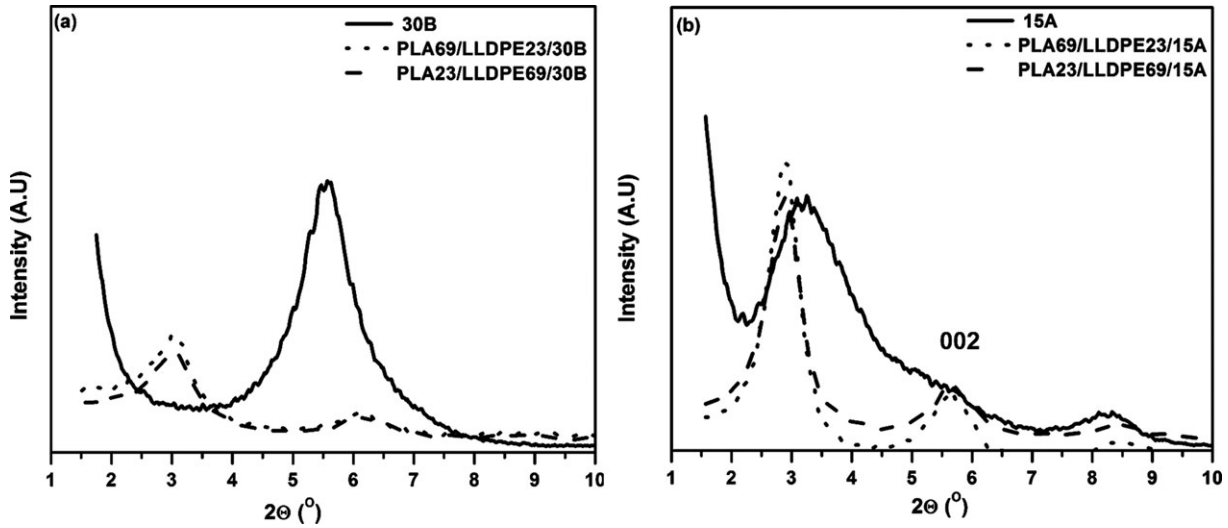

Figure 1. XRD patterns of various PLA/LLDPE mixtures: (a) Cloisite 30B and 30B-based nanocomposites, (b) Cloisite 15A and 15A-based nanocomposites.

melts at temperature significantly lower (approximately at 75°C) than the other two polymers, it encompasses the 30B nanoparticles preferentially.

The TEM micrographs of PLA69/LLDPE23/15A-based nanocomposites are shown in Figure 2(d–f). As it can be seen organoclay is localized mainly at the interface. However, in 15A-based nanocomposites, as earlier confirmed by XRD results, unlike the 30B based nanocomposites, the level of exfoliation is lower and some large tactoids are observable at the interface of PLA and LLDPE. The main reason behind this might be the lesser affinity of 15A modifier with compatibilizer and PLA phase. Significant difference is not observed between the localization of organoclays in 30B and 15A-based nanocomposites. In both systems, the nanoclays are localized mainly at the

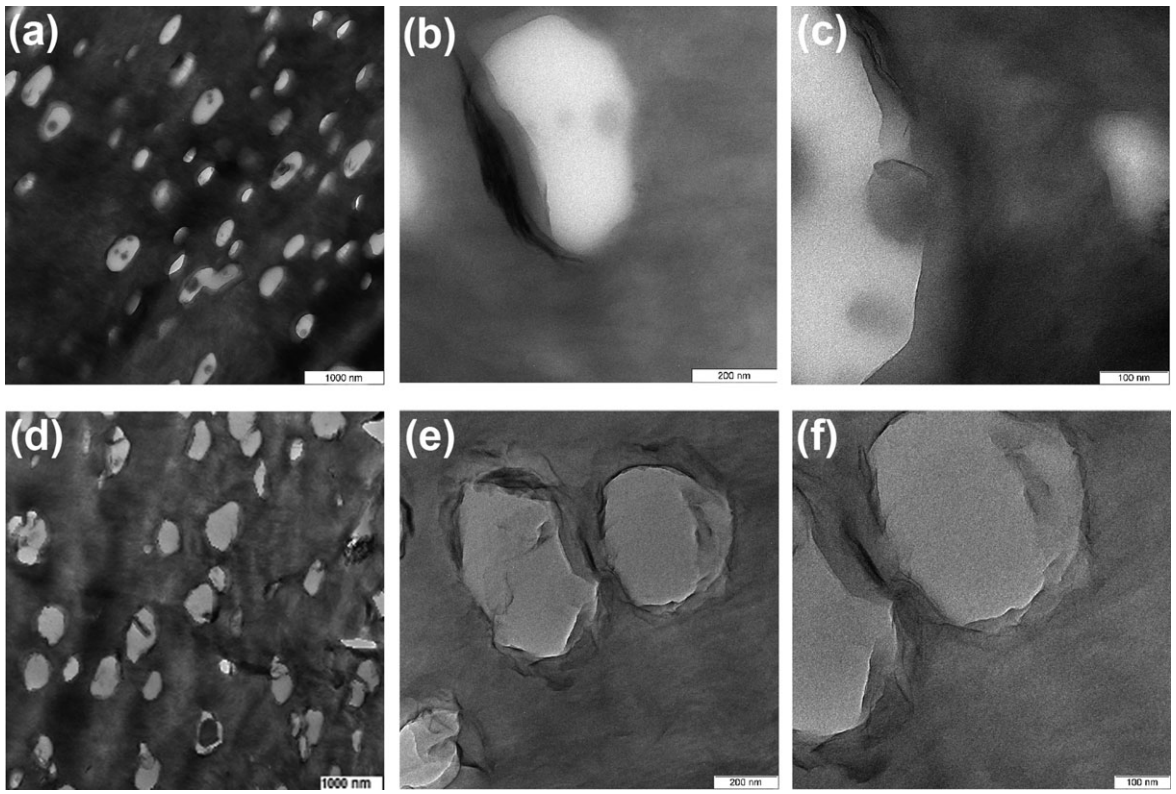

Figure 2. The TEM micrographs of various compatibilized PLA/LLDPE nanocomposites, (a–c) PLA69/LLDPE23/30B, (d–f) PLA69/LLDPE23/15A.

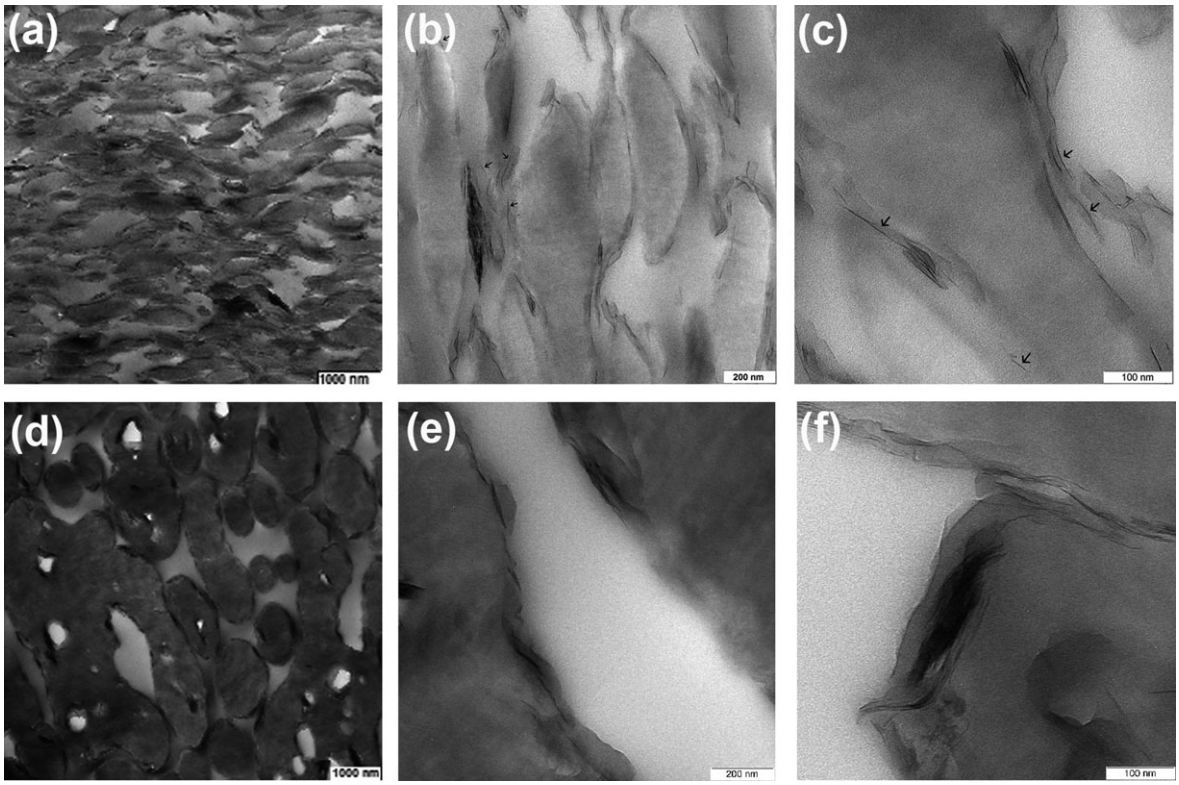

Figure 3. TEM Micrographs of various compatibilized PLA/LLDPE nanocomposites (a–c) PLA23/LLDPE69/30B, (d–f) PLA23/LLDPE69/15A.

interface. However, in 30B-based nanocomposites some parts of nanoclays are localized in PLA phase.

Figure 3 shows the TEM micrographs of LLDPE-rich system. Similar to the PLA-rich system both 30B and 15A organoclays are localized mainly at the interface of PLA and LLDPE. It is interesting to underline that in spite of higher affinity between LLDPE and 15A, no localization of this organoclay within LLDPE phase are observed in LLDPE and PLA-rich system. One possible reason for this behavior is due to the easier diffusion of the compatibilizer chain around and into the nanoclay aggregates at the initial stage of melt mixing. On the other hand, most of the nanoclays have a tendency to be further dispersed on the phase interface driven by the mixing flow because the carboxylic group of modifier on surface of the nanoclays has good affinity to both the PLA and the compatibilizer phases. As it can be seen from Figure 3 in LLDPE-rich system some parts of exfoliated clay (both 30B and 15A) platelets are located at the interface between PLA and LLDPE. However, in both PLA and LLDPE-rich systems the overall organoclay distribution is better for 30B than the equivalent 15A composites.

Comparing the dispersion of these nanocomposites at different PLA contents one can conclude that the influence of PLA concentration on localization and the state of dispersion is not significant. This can also be an effect of addition of all the components to the extruder simultaneously. In such case the phase which melts at temperature significantly lower than other phases encompasses the organoclays preferentially. This interfacial localization of the nanoclays could prevent the coalescence of the dispersed phase effectively which helps compatibilization during melt mixing. Therefore, both the thermodynamically and kinetically driven compatibility is possible to occur.[29,30] Such interface localization of the nanoclays, as a result, improves the interfacial adhesion of the PLA/LLDPE blend matrix evidently as confirmed by the SEM micrographs presented in Figures 4 and 5.

EM micrographs of the cryofracture surfaces provide morphological information complementary to the TEM results. The corresponding SEM micrographs of the cryofracture surface along the longitudinal (flow) direction for the neat as well as the nanoclay-filled blends, for PLA-rich and LLDPE-rich systems, are presented in Figures 4 and 5, respectively. From Figure 4, it is seen that all PLA-rich samples have typical droplet-in matrix morphologies where some of the LLDPE inclusions are deformed in to ellipsoids due to the high shear flow in the injection molding process. A significant change in the blend phase morphology is seen on addition of a small amount of organoclay. As it can be seen in case of PLA/LLDPE/30B system [Figure 4(b)], the fracture surface appears coarser due to size reduction of dispersed phase.[19] It is to be noted that the fracture surfaces may have also been an effect of sample preparation conditions and the locations where the specimens are taken from. In comparison with 30B, due to less affinity of 15A towards compatibilizer and PLA, the reduction of the dispersed phase is less than the corresponding 30B composites (comparing Figure 4(b,c)]. On the other hand, localization of some extent of organoclay at the interface of the blend is one of the

Applied Polymer SCIENCE

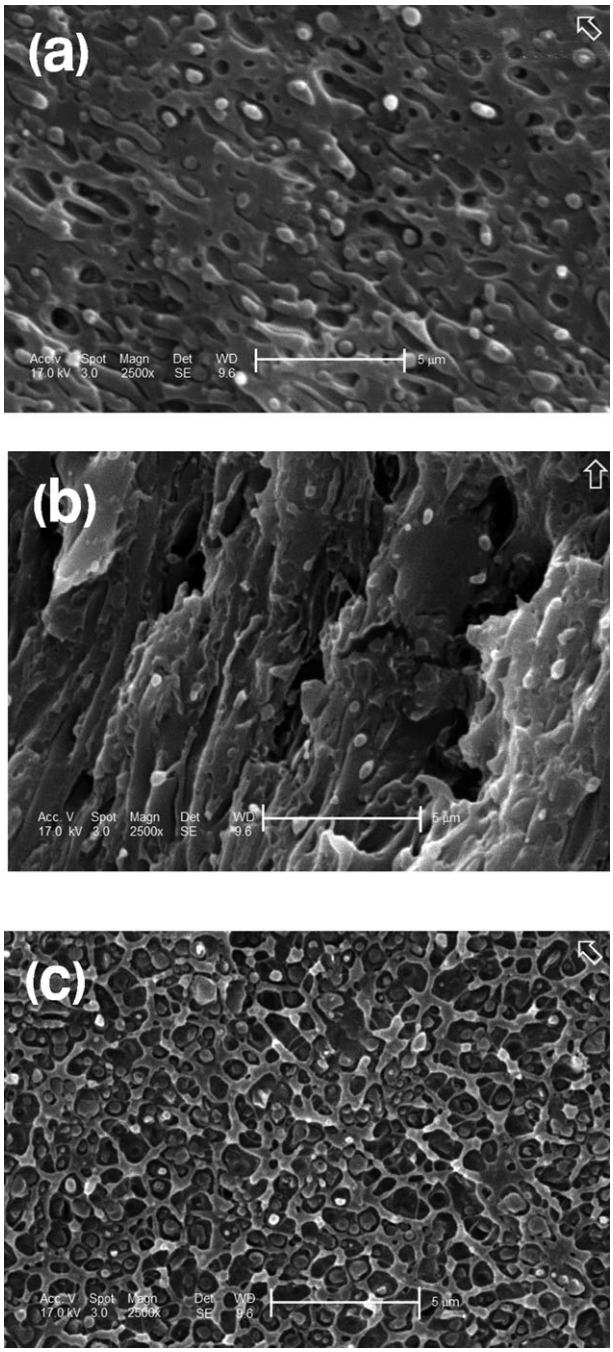

Figure 4. SEM micrographs of cryofractured compatibilized PLA69/LLDPE23 system before stretching, PLA/LLDPE, (b) PLA/LLDPE/30B, (c) PLA/LLDPE/15A.

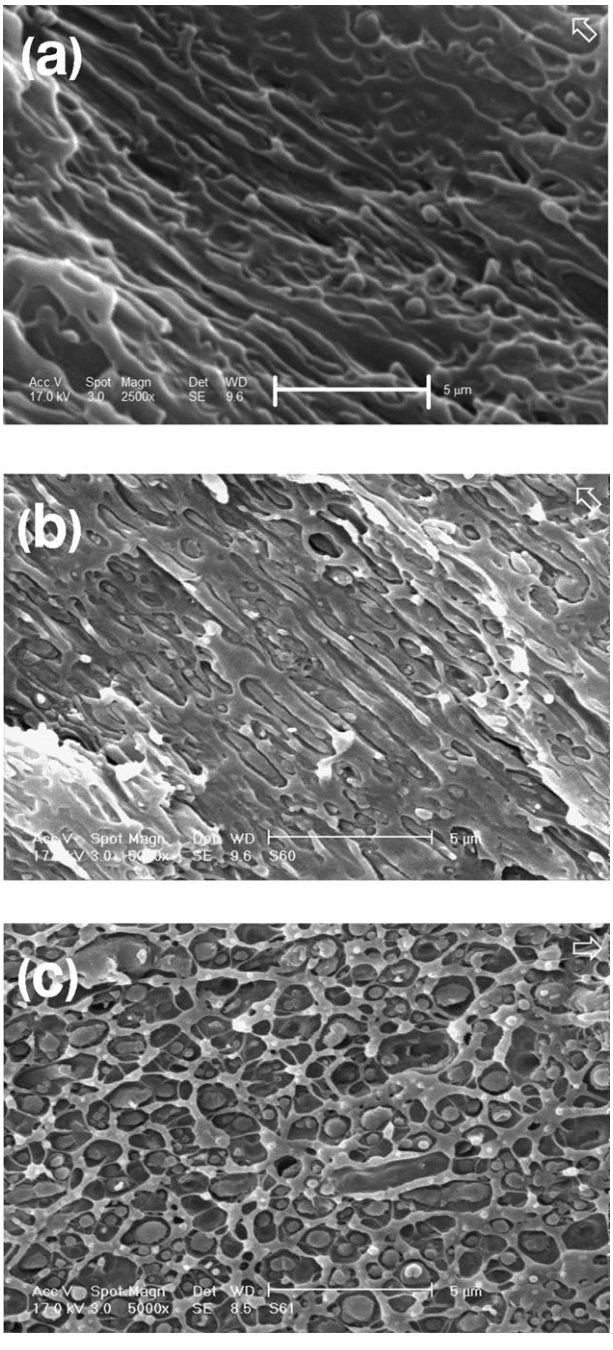

Figure 5. SEM micrographs of cryofractured PLA23/LLDPE69 system (LLDPE-rich) before stretching, PLA/LLDPE, (b) PLA/LLDPE/30B, (c) PLA/LLDPE/15A.

equisetic mechanisms of size reduction of the dispersed phase.[23–26]

Figure 5 shows the phase morphology of LLDPE-rich system with and without clay loading. Strong interfacial bonding between PLA and LLDPE is not observed in this compatibilized system which is an indication of an interfacial debonding between PLA and LLDPE phases. All the samples exhibit co-continuous morphology.

As it can be seen from Figures 4 and 5 based on different contents of PLA/LLDPE, there is a significant difference in break morphology of blend. Decreasing the PLA content changes the morphology from a droplet-in matrix to a coarse co-continuous. It is well known that there can be a co-continuous region around the phase inversion composition whose composition range depends mainly on the interfacial tension.[21]

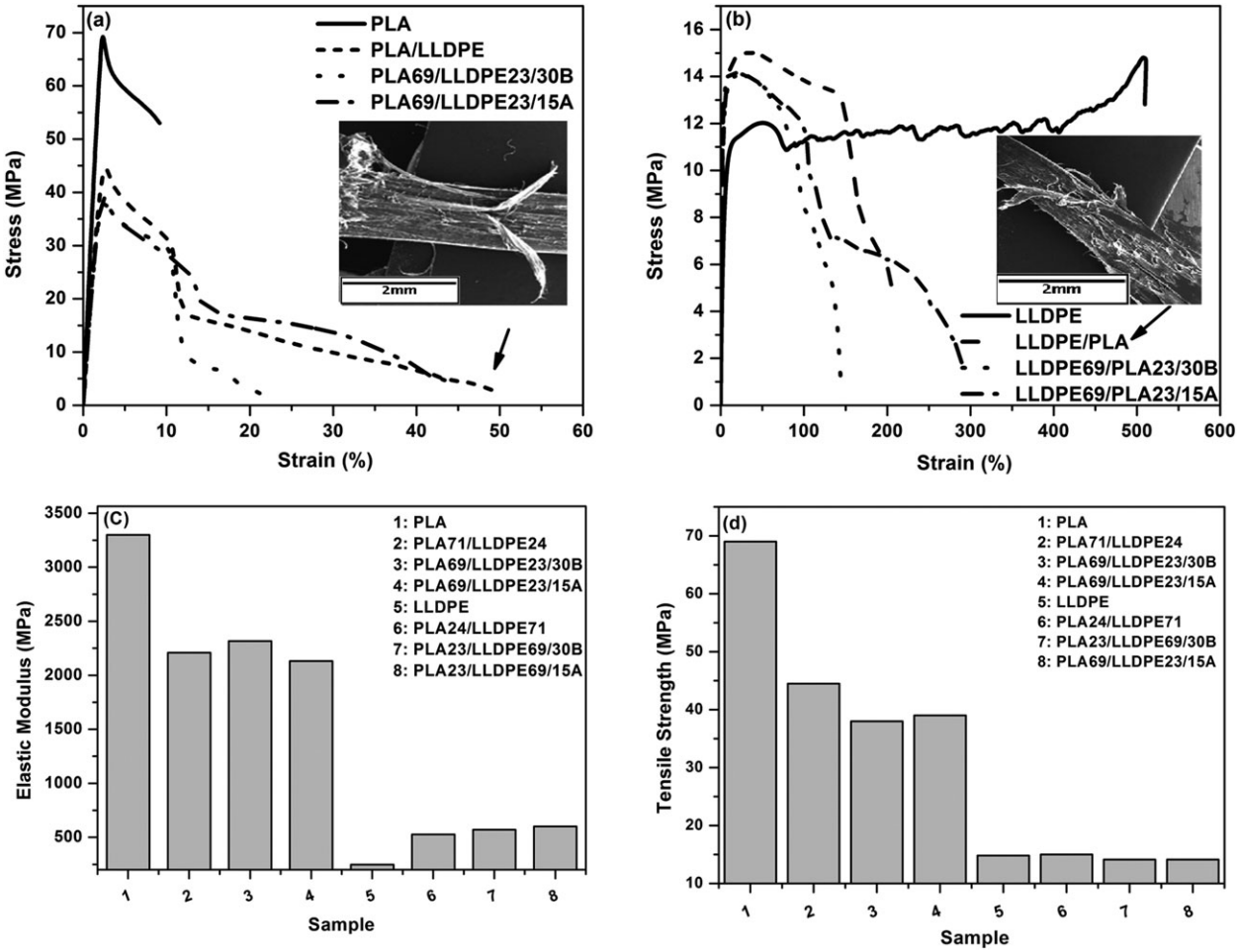

Figure 6. Tensile properties of (a) PLA-rich system, (b) LLDPE-rich system, (c) Tensile modulus, (d) Tensile strength.

In the case of PLA/LLDPE/15A with different PLA contents the size of dispersed phase is bigger than the corresponding nanocomposites made from 30B. This can be attributed to the localization of the major parts of organoclay particles at the interface (Figures 2 and 3). It appears that more polar structure of the 30B modifier is responsible for enhanced interactions with compatibilizer and PLA. This modification of the interfacial tension affects the breakup/coalescence equilibrium in favor of the breakup and should lead to smaller drops.

From Figures 4 and 5 it is also seen that by incorporation of 15 A to both PLA-rich and LLDPE-rich blend systems the phase morphology significantly changes from elongated dispersed domains to somehow more spherical domains. Such phenomenon was not observed in the 30B-based systems. The observed great change in phase morphology as compared with the 30B-based samples can be attributed to the difference in interaction of compatibilizer with 15A and 30 B in the respective systems. Considering the cationic nature of 30B modifier as compared to nonpolar modifier of 15 A it is expected that 15A should have less interaction with the compatibilizer as compared with 30B and therefore it might be more free to affect the blend phase morphology. On the other hand, since this change of phase morphology by presence of 15A is evident in both PLA-rich and LLDPE-rich system the change in morphology can not be due to the difference in type of matrix.

Tensile Properties

Figure 6 presents the tensile properties (stress–strain curves, tensile modulus and tensile strength) of PLA-rich and LLDPE-rich blends and nanocomposites. The tensile data are summarized at Table II. From these results the effect of addition of LLDPE and organoclay on tensile properties can be seen clearly. LLDPE can convert the brittle PLA to a flexible material on expense of a large strength lost. Addition of 23% LLDPE to PLA reduces the tensile strength and modulus by about 60%. In contrast the elongation at break increases significantly (about 5-folds). This exhibits the toughening effect of LLDPE on PLA. The increase of modulus and the decrease of elongation at break in LLDPE-based system, as compared with neat LLDPE can also be attributed to inherent brittle nature of PLA. The organoclay role on modulus enhancement can be seen from Figure 6(c). The modulus of the neat PLA/LLDPE blend increases to some extent by inclusion of 3% 30B. These changes can be explained by the preferential localization of the organoclay (30B) at interface and the degree of exfoliation which described

Table II. Elastic Modulus and Elongation at Break of PLA/LLDPE Composites

Samples	E_t (MPa)	Standard deviation (MPa)	ε_B (%)	Standard deviation (%)
PLA	3338	58.7	9.2	2.7
LLDPE	248	3.41	509.5	34.7
PLA71/LLDPE24/ Elvaloy PTW	2208	187.9	50.3	14.3
PLA69/LLDPE23/ Elvaloy PTW/ 30B	2220	49.7	21.8	4
PLA69/LLDPE23/ Elvaloy PTW/ 15A	2132	71.2	47.2	2.3
PLA24/LLDPE71/ Elvaloy PTW	526	14.8	206.9	43.2
PLA23/LLDPE69/ Elvaloy PTW/ 30B	571	22.9	144.8	26.5
PLA23/LLDPE69/ Elvaloy PTW/ 15A	599	15.5	257.5	54.2

All blend nanocomposites contain 3 wt % nanoclay and 5 wt % compatibilizer.

earlier (TEM micrographs). Based on the other researcher's report, the mechanical properties of nanocomposites are sensitive to the level of exfoliation and localization of nanoclays.[27] In general, the addition of nanoclays in a polymer matrix results in significant improvements of modulus. However, exceptions to this general trend have been reported.[27] In addition the improvement of the modulus was observed by incorporating clay in the matrix.[27] As it can be seen in Figures 2 and 3, most of the nanoclays were localized at the interface. This localization of nanoclay may have influence on the improvement of the mechanical properties. In addition in both PLA and LLDPE-rich system, silicate layers are intercalated at the interface and only a few exfoliated layers are observable. In this case the improvement of tensile properties is not significant by the addition of nanoclays.

In general, the addition of an organically modified layered silicate in a polymer matrix results in significant improvements of mechanical properties. However, exceptions to this general trend have been reported. The level of exfoliation and localization of organoclays are two crucial factors which affect the degree of improvement of mechanical properties. Mixing methods has a significant effect on the level of exfoliation and localization of organoclays. In this study due to simultaneous addition of the components, the organoclays localized at the interface in both PLA and LLDPE-rich systems. The results show that due to the low level of exfoliation of organoclay and localization of organoclays at the interface the improvement of mechanical properties is not significant. As the localization of organoclays at the matrix has major role on the improvement of mechanical properties, through a proper mixing method the organoclays can be localized in matrix, in such case the effect of organoclays on the properties would be significant. In our previous work,[23] the effect of mixing methods on the morphology and properties of PLA/LLDPE was investigated.

In the case of PLA/LLDPE/15A with different PLA contents, the enhancement of the modulus was observed only in specimen with higher content of LLDPE [see Figure 6(a,c)]. There are several factors which can contribute to the modulus enhancement. The first and the major contribution are exerted from the exfoliated and/or intercalated organoclay layers with their high inherent modulus. Second, the formation of a network-like co-continuous morphology which in turn can contribute to the modulus enhancement. The role of co-continuous morphology in enhancement of modulus is evident if one compares the modulus of two PLA/LLDPE blend nanocomposites with a similar clay type but at higher and lower contents of LLDPE. As it was seen from the SEM micrographs presented in Figures 4 and 5 reduction of PLA content changed the morphology from droplet-in matrix to co-continuous. In other words the comparison of the effects of 15A and 30B on the enhancement of modulus can reveal the affinity between PLA matrix and 30B. In contrast the tensile strength as well as elongation at break of the PLA/LLDPE/30B blend nanocomposite at different contents of PLA show decreasing trend. Similar behavior was observed for the equivalent 15A nanocomposites.

This could be due to the presence of some organoclay stacks (see Figures 2 and 3) and high stress concentration which led to large voids during the tension test. These voids develop into cracks and reduce elongation at break. It is well known that obtaining exfoliated nanocomposites without any agglomeration is very difficult by melt compounding. In addition tensile strength and elongation at break are much more affected by the interfacial adhesion than modulus. It was evident from the morphological studies that strong interfacial bonding was not effectively established by the compatibilizer and addition of organoclay. The stepwise drops in stress–strain curves [see Figure 6(a,b)] indicates a sequential fracture behavior during tension testing for PLA/LLDPE blends and their nanocomposites at different contents of PLA. The SEM micrographs from the tensile-fracture surface presented as insets in Figure 6(a,b) exhibit a multilayer structure of the specimens and sequential fracture behavior. Because of the cooling and shear gradient across the part thickness, the injection molded polymer parts often exhibit a multilayer structure.[29,30] The multilayer structure can be divided into skin and core layers. The orientation of polymer chains in core layer is less than skin layer. This characteristic is caused by lower shear rate, lack of extensional flow, and longer cooling time in the core layer.[31]

Figure 7 shows the SEM micrographs of the binary blends and their nanocomposites after the tension test. All the samples were cryo-fracture along the longitudinal direction i.e. tensile direction. The multilayer structure of PLA/LLDPE blend and nanocomposites can be easily distinguished from these micrographs. Because of high shear rate and extensional flow in injection molding, polymer chains are aligned and the inclusions become smaller. As it can be seen from Figure 7 the morphology changes during the tension test. Because of

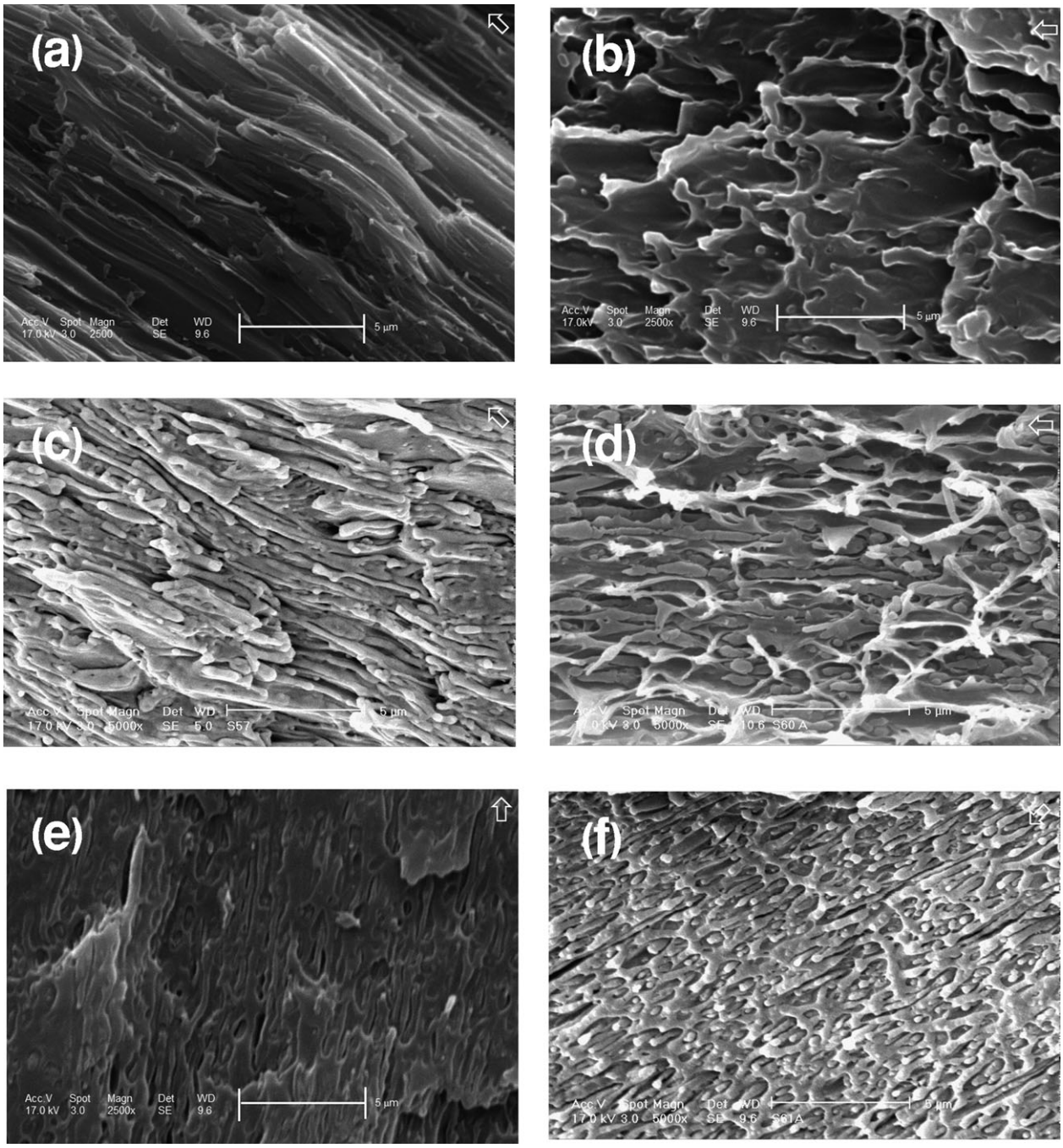

Figure 7. SEM micrographs of PLA/LLDPE and their nanocomposites after stretching: (a) PLA69/LLDPE23, (b) PLA23/LLDPE69, (c) PLA69/LLDPE23/30B, (d) PLA23/LLDPE69/30B, (e) PLA69/LLDPE23/15A, (f) PLA23/LLDPE69/15A. Arrows indicate tensile direction.

the toughening effect of LLDPE and compatibilizing role of organoclay, binary blend of PLA/LLDPE and their nanocomposites show different morphology after stretching. Due to brittle behavior of PLA, PLA/LLDPE blend, and nanocomposites with higher content of PLA show smoother surfaces than samples with lower content of PLA. It is clearly seen that the ductility of fracture surface is the most excessive in samples with higher content of LLDPE. During the tensile test all blend nanocomposites, showed obvious stress whitening. In other word as shown in Figure 7, the PLA matrix in the PLA-based blend and nanocomposites demonstrates intensive fibrillation due to the release of strain constraints initiated by interfacial debonding between PLA and LLDPE. Similar results have been reported by other researchers.[20] According to multiple crazing theory, interfacial adhesion, particle size, size distribution, and content of dispersed phase all have a significant effect on the final mechanical properties of blend nanocomposites.[32–34]

CONCLUSIONS

The compatibilized blend nanocomposites based on PLA/LLDPE/nanoclay were successfully prepared by melt extrusion process. The influence of type of clay on the morphology and mechanical properties of two PLA-rich and LLDPE-rich blend systems was investigated. Investigation on the effect of organoclay type and blend composition on the microstructures and mechanical properties of PLA blend nanocomposites showed that the overall organoclay distribution was better for the 30B than the equivalent 15A composites. Similar diffraction peaks were observed for different PLA contents indicating that the ability of PLA and LLDPE matrices to expand the organoclay crystallites was similar. The results indicate that decreasing the PLA content changed the morphology from droplet-in matrix to coarse co-continuous in both systems. Moreover, in the case of PLA/LLDPE/15A with different PLA content, the size of dispersed phase was increased in comparison with the equivalent 30B nanocomposites. The mechanical properties revealed that the addition of LLDPE to PLA results in a large modulus lost and elongation improvement. A layered structure and stress whitening were noted in the injection-molded specimens. In contrast, by addition of both types of organoclays to PLA/LLDPE blend the tensile strength as well as elongation at breaks showed decreasing trend for both PLA-rich and LLDPE-rich systems. This could be due to some organoclay stacks and high stress concentration which led to large voids during the tension test. It was shown that the modulus enhancement in nanocomposites with co-continuous morphology was much higher than that with droplet-in matrix.

ACKNOWLEDGMENTS

The authors thank Uta Reuter, Mechanical laboratory of IPF Dresden for her technical helps. Also technical supports from XRD and Microscopic lab of IPPI (Iran) are highly appreciated.

REFERENCES

1. Mohanty, A. K.; Misra, M.; Drzal, L. T.; Natural Fibers, Biopolymers, and Biocomposites, Taylor Francis Group LLC, **2005**, 1st Edition, London.
2. Ray, S. S.; Bousmina, M. *Prog. Mater. Sci.* **2005**, *50*, 962.
3. Shibata, M.; Teramoto, N.; Inoue, Y. *Polymer* **2007**, *48*, 2768.
4. Anderson, K. S.; Lim, S. A.; Hillmyer, M. A. *J. Appl. Polym. Sci.* **2003**, *89*, 3757.
5. Kim, Y. F.; Choi, C. N.; Kim, Y. D.; Lee, K. Y.; Lee, M. S. *Fiber. Polym.* **2004**, *5*, 270.
6. Wang, Y.; Hillmyer, M. *J. Polym. Sci. Part A: Polym. Chem.* **2001**, *39*, 2755.
7. Rezgui, F.; G'Sell, C.; Dahoun, A.; Hiver, J. M.; Sadoun, T. *Polym. Eng. Sci.* **2011**, *5*, 117.
8. Rezgui, F.; G'Sell, C.; Dahoun, A.; Hiver, J. M.; Sadoun, T. *Polym. Eng. Sci.* **2011**, *5*, 126.
9. Nuñez, K.; Rosales, C.; Perera, R.; Villarreal, N.; Pastor, J. M. *Polym. Eng. Sci.* **2012**, *52*, 988.
10. Singh, G.; Bhunia, H.; Rajor, A.; Choundhary, V. *Polym. Bull.* **2011**, *66*, 939.
11. Singh, G.; Navleen, K. B.; Haripada, B.; Pramod, K. B.; Uttam, K. M. *J. Appl. Polym. Sci. 124*, **2011**, 1993.
12. Raghavan, D.; Emekalam, A. *Polym. Degrad. Stabil.* **2001**, *72*, 509.
13. Cabedo, L.; Feijoo, J. L.; Villanueva, M. P.; Lagaron, J. M.; Gimenez, E. G. *Macromol. Symp.* **2006**, *233*, 191.
14. Yu, Z.; Yin, J.; Yan, S.; Xie, Y.; Ma, J.; Chen, X. *Polymer* **2007**, *48*, 6439.
15. Wu, D.; Zhang, Y.; Zhang, M.; Yu, W. *Biomacromolecules* **2009**, *10*, 417.
16. Shafiei Sabet, S.; Katbab, A. A. *J. Appl. Polym. Sci.* **2009**, *111*, 1954.
17. Chen, G. X.; Kim, H. S.; Kim, E. S.; Yoon, J. S. *Polymer* **2005**, *46*, 11829.
18. Chen, G. X.; Yoon, J. S. *Polym. Degrad. Stabil.* **2005**, *88*, 206.
19. Bhatia, A.; Gupta, R. K.; Bhattacharya, S. N.; Choi, H. J. *J. Appl. Polym. Sci.* **2009**, *114*, 2837.
20. Ko, S. W.; Hong, M. K.; Park, B. J.; Gupta, R. K.; Choi, H. J.; Bhattacharya, S. N. *Polym. Bull.* **2009**, *63*, 125.
21. Ko, S. W.; Gupta, R. K.; Bhattacharya, S. N.; Choi, H. *J. Macromol. Mater. Eng.* **2010**, *295*, 320.
22. Jiang, L.; Liu, B.; Zhang, J. *Ind. Eng. Chem. Res.* **2009**, *48*, 7594.
23. As'habi, L.; Jafari, S. H.; Khonakdar, H. A.; Boldt, R.; Wagenknecht, U.; Heinrich, G. *Exp. Polym. Lett.* **2013**, *7*, 21.
24. Fenouillot, F.; Cassagnau, P.; Majeste, J. C. *Polymer* **2009**, *50*, 1333.
25. A'shabi, L.; Jafari, S. H.; Khonakdar, H. A.; Baghaei, B. J. *Polym. Res.* **2011**, *18*, 197.
26. Lai, S. M.; Liao, Y. C.; Chen, T. W. *J. Appl. Polym. Sci.* **2006**, *100*, 1364.
27. Pavlidou, S.; Papaspyrides, C. D. *Prog. Polym. Sci.* **2008**, *33*, 1119.
28. Lee, S., H.; Youn, J. R. *J. Appl. Polym. Sci.* **2008**, *109*, 1221.
29. Jafari, S. H.; Pötschke, P.; Stephan, M.; Warth, H.; Alberts, H. *Polymer* **2002**, *43*, 6985.
30. Steinmann, S.; Gronski, W.; Friedrich, C. *Rheol Acta.* **2002**, *41*, 77.
31. Fellahi, S.; Favis, B. D.; Fisa, B. *Polymer* **1996**, *37*, 2615.
32. Konishi, Y.; Cakmak, M. *Polymer* **2005**, *46*, 4811.
33. Li, Z. M.; Yang, W.; Yang, S.; Huang, R.; Yang, M. B. *J. Mater. Sci.* **2004**, *39*, 413.
34. Bucknall, C. B. Toughened Plastics; Applied Science Publishers Ltd: London, **1977**; p 189.